International Journal of Innovative Computing, Information and Control
Volume **14**, Number **2**, April **2018**

ICIC International ©2018 ISSN 1349-4198
pp. **671–681**

ROTOR LEVITATION AND VIBRATION CONTROL OF HYBRID POLE BSRM USING FUZZY SLIDING MODE CONTROLLER

Polamraju Venkata Subrahmanya Sobhan[1]
Gundavarapu Venkata Nagesh Kumar[2]
and Pulipaka Venkata Ramana Rao[3]

[1]Department of Electrical and Electronics Engineering
Vignan's Foundation for Science, Technology and Research
Vadlamudi, Guntur 522213, India
pvssobhan@gmail.com

[2]Department of Electrical and Electronics Engineering
Vignan's Institute of Information Technology
Visakhapatnam 530049, India
drgvnk14@gmail.com

[3]Department of Electrical and Electronics Engineering
Acharya Nagarjuna University
Guntur 522510, India
pvr_eee@yahoo.co.in

Received June 2017; revised October 2017

Abstract. *Rotor vibration control during startup, acceleration and deceleration phases is one of key problems besides stable levitation, in high-speed applications of bearingless switched reluctance motor (BSRM). The use of linear control strategies alone is not effective in suppressing vibration due to residual unbalance and external disturbance. This paper presents implementation of a nonlinear control method by integrating the features of fuzzy logic and the sliding mode control (SMC) to minimize the rotor vibration and eccentricity error of BSRM. The application of fuzzy SMC with the independent control of the radial force and rotational force guarantees stable levitation as well as the vibration reduction and the same is demonstrated with experimental results.*
Keywords: BSRM, Radial force control, Fuzzy sliding mode controller, Rotor eccentricity

1. **Introduction.** High speed motors working in harsh environments such as high temperatures, radiation and poisonous substances are limited because of motor breakdown due to vibrations of mechanical bearings. The concept of magnetic bearings is an alternative to the issues of slide or ball bearings because of its advantages of friction-free, negligible thermal problems, and lubrication free. A magnetic bearing is an electro-mechanical element which levitates the rotor magnetically without any mechanical contact between the stator and rotor [1,2].

A bearingless motor integrates the functions of rotation and noncontact levitation and they are employed in high-speed and high-purity areas such as semiconductor, radioactive, space equipment pharmaceutical and medical industry [3-8]. Due to the single-excited, doubly salient structure and presence of significant magnetic force between rotor and stator poles, the switched reluctance motors are ideally suitable as bearingless motors. The non uniform and short air-gap adequately generate torque and radial force to levitate the rotor [9].

Many designs are proposed for the bearingless switched reluctance motor (BSRM) having separate windings for radial force and torque to minimize the interactions between the flux generated by both windings. A control scheme incorporating auxiliary winding for rotor levitation in stator poles along with torque winding was proposed by M. Takemoto et al. [10-12]. In the new structure of single winding BSRM proposed by L. Chen and W. Hofmann, three radial forces and three torques are produced by three winding currents in each commutating period [13,14]. In the hybrid structure introduced by C. R. Morrison et al., the rotor has two types of laminations. The circular type is for improving radial force and the multi pole type is for conventional motoring [15,16]. One critical issue in the structures mentioned is the control of radial force which is tightly coupled with torque control and is unwanted for high speed applications due to uncontrolled rotor vibrations. To tackle the coupling issue, a hybrid stator pole structure is proposed by H. Wang et al., with two separate poles and windings for both rotor levitation and motoring [17,18]. The torque pole produces torque and the radial force pole having arc greater than the torque pole arc produces the necessary radial force. However, under normal working conditions there exists less degree of coupling between the two fluxes; hence the radial force control of the hybrid BSRM is quite a challenging problem [19]. Z. Xu et al. proposed one PI controller for speed control and two independent PID controllers for controlling the rotor radial displacement in both directions (x and y); however, the tuning of the PID controller parameters tuning is a tedious task [20].

The execution of vibration control scheme for BSRM relies on the control of radial force and rotational force which are strongly coupled and impacted by the currents in radial force and torque windings, the rotor position, electrical and mechanical parameters of the motor [21,22]. Moreover, presence of large ripples in the radial force and torque deteriorates the performance.

The nonlinear vibrations due to the nonlinearity of the radial force, the presence of residual imbalance uncertainty and parameter variations in BSRM structure, complicates controller design [23]. Therefore, SMC is an appropriate robust control strategy. In order to control rotor vibration and speed in finite time, the fast reaching mode with a high gain control is advisable but this prompts increment in chattering. In this study, a fuzzy based sliding mode controller is proposed for BSRM drive and the fuzzy logic is used to adjust the sliding line parameters to avoid chattering. The proposed controller modifies the signum function of switching control term with fuzzy logic function, to eliminate rotor vibrations (chattering) with assured robust levitation control under load variations and disturbances. The validity of the proposed control algorithm is affirmed by a Matlab/Simulink software and a prototype BSRM drive with a TMS320F2812 DSP. Experimental results confirm that the proposed controller ensures a better performance over the conventional SMC method having motor parameter uncertainties and external disturbances.

The organization of this paper is as follows. In the following section, the constructional features, the winding structure and the principle of torque and levitation control of the prototype hybrid BSRM are presented. The design procedure of the proposed fuzzy sliding mode controller, torque and radial force control of the BSRM is explained in Section 3. Section 4 demonstrates the experimental test setup of the proposed control technique with TI TMS320F2812 DSP and results analysis. The last section gives conclusion got from this work.

2. **Hybrid Pole Type BSRM: Structure and Operation.**

2.1. **BSRM structure.** Figure 1 shows the pole structure of 12/14 hybrid BSRM with 12 poles on stator and 14 poles on rotor. The stator includes two different windings on

poles, i.e., four windings P_{xp}, P_{xn}, P_{yp} and P_{yn} for radial force generation with currents i_{xp}, i_{xn}, i_{yp} and i_{yn} respectively and the other eight windings are for torque generation to operate as a two phase SRM. Four windings P_{A1}-P_{A4} are connected in series and excited simultaneously to form phase A and similarly, windings P_{B1}-P_{B4} form phase B. The rotor poles are symmetrically spaced without windings. The four radial force poles and the two torque winding phases are placed coordinately and diagonally respectively and all are excited individually. This hybrid pole structure totally decouples the radial force control from torque control because of the negligible and undesirable torque produced by radial force poles.

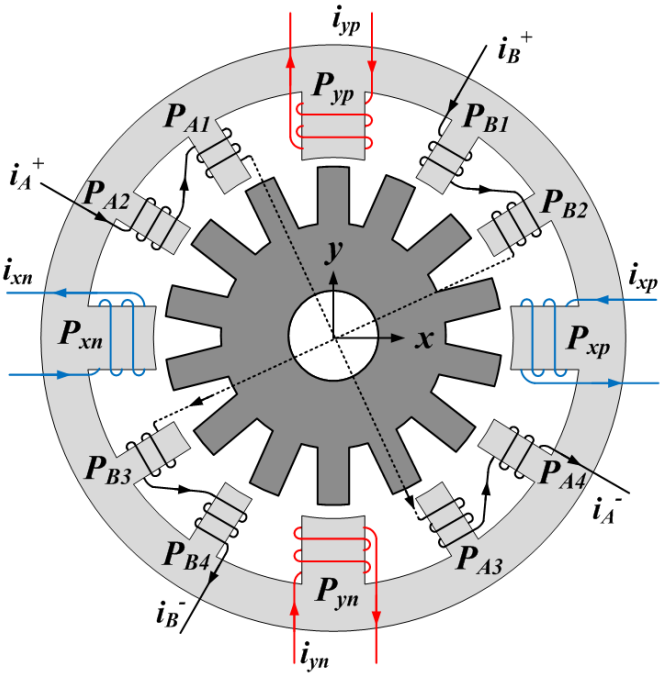

FIGURE 1. Basic structure of 12/14 BSRM

2.2. **Torque control.** The electromagnetic torque produced in BSRM mainly depends on winding inductance profile and expressed as

$$T = \frac{1}{2} i^2 \frac{dL}{d\theta} \tag{1}$$

where i and L are current and inductance of torque or radial force windings, and θ is the rotor position. In radial force windings, the torque contribution is negligible because of constant inductance profile for constant current; hence, the torque is independent of radial force current. In the torque winding, due to large variation in the inductance profile from aligned to unaligned position, the slope of inductance is very large; hence, the net torque on the rotor is due to torque windings only.

The torque, thereby the rotor speed control can be achieved by synchronizing the phase winding currents i_A and i_B with the rotor position by controlling the PWM duty ratio to turn on and turn off of switches in asymmetric converters of corresponding torque winding phase as shown in Figure 2.

2.3. **Radial force control.** The generated radial force in the x-direction is due to the currents i_{xp} and i_{xn}, and in y-direction is due to currents i_{yp} and i_{yn} flowing in four radial force poles P_{xp}, P_{xn}, P_{yp} and P_{yn}. The radial force on the rotor in any position

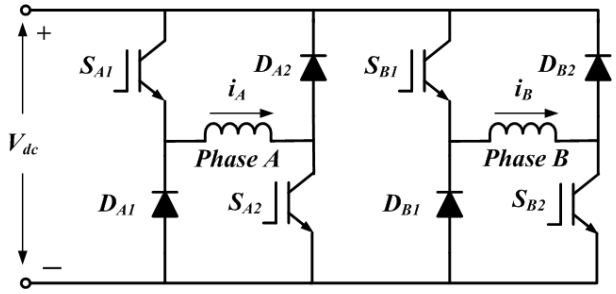

FIGURE 2. Asymmetric converter for torque windings

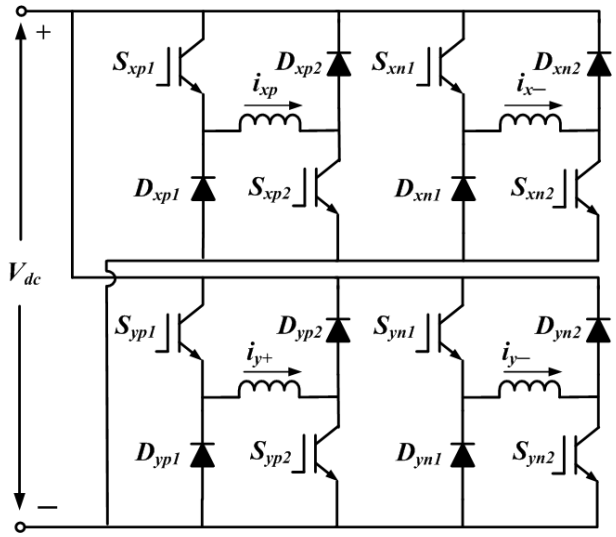

FIGURE 3. Asymmetric converter for radial force windings

and directions ($+x$, $-x$, $+y$ and $-y$) can be controlled by controlling i_{xp}, i_{xn}, i_{yp} and i_{yn} independently. Based on the rotor eccentric position, any two levitation windings are selected accordingly and controlled independently by asymmetric bridge converter shown in Figure 3.

3. **Fuzzy Sliding Mode Control.** The sliding mode control strategy with features such as robustness, quick convergence and high control precision, is widely implemented in different systems. However, its significant drawback is the chattering problem for practical applications. Fuzzy control (FC) is especially reasonable for those systems with modeling complexities and uncertainties. The extensive uncertainties cause high chattering and to eliminate it the SMC need high switching gain with an increased boundary limits. However, the continuous increase in the boundary limits leads to ineffective sliding mode system. The alternative control scheme is to combine the effects of fuzzy control and SMC known as FSMC to have an effective control.

3.1. **Sliding mode control.** The SMC strategy utilizes discontinuous control to drive state trajectories towards a particular hyperplane in the state space, and to keep them up sliding on the hyperplane until stable equilibrium state is reached.

An nth-order uncertain nonlinear system is represented as:

$$\begin{aligned} \dot{x}_i &= x_{i+1} \\ \dot{x}_n &= \hat{f}(\mathrm{x}) + \Delta\hat{f}(\mathrm{x}) + \eta(t) + \hat{g}(\mathrm{x})u(t) \\ y &= x_1 \end{aligned} \tag{2}$$

where $\mathrm{x} = \begin{bmatrix} x_1 & x_2 & \dots & x_n \end{bmatrix}^{\mathrm{T}} = \begin{bmatrix} x & \dot{x} & \dots & x^{(n-1)} \end{bmatrix}^{\mathrm{T}}$ is the state vector, $u(t)$ is the control signal, $y = x_1$ is the system output, $\hat{f}(\mathrm{x})$ and $\hat{g}(\mathrm{x})$ are nonlinear functions, $\Delta\hat{f}(\mathrm{x})$ is the uncertainty of unmodeled dynamics and $\eta(t)$ is the disturbance.

$$\left\|\Delta\hat{f}(\mathrm{x})\right\| \leq \varepsilon \text{ and } \|\eta(t)\| \leq \gamma \tag{3}$$

where ε, γ are positive constants.

The desired state trajectory is defined by $\mathrm{x}_r^T = \begin{bmatrix} x_r & \dot{x}_r & \dots & x_r^{(n-1)} \end{bmatrix}$, then the tracking error is defined by $\mathrm{e} = \mathrm{x} - \mathrm{x}_r = \begin{bmatrix} e & \dot{e} & \dots & e^{(n-1)} \end{bmatrix} = \begin{bmatrix} e_1 & e_2 & \dots & e_n \end{bmatrix}$ and

$$\dot{e}_n = x^{(n)} - x_r^{(n)} = \hat{f}(\mathrm{x}) + \Delta\hat{f}(\mathrm{x}) + \eta(t) + \hat{g}(\mathrm{x})u(t) - x_r^{(n)} \tag{4}$$

The sliding function is defined as

$$s = \sum_{i=1}^{n-1} k_i\, e_i + e_n \tag{5}$$

where k_i, $i = 1, 2, \dots, n-1$ are positive constants which make the zeros of the polynomial $\lambda^{n-1} + k_{n-1}\lambda^{n-2} + \cdots + k_2\lambda + k_1$ are in the left side of the imaginary axis in the complex plane and the choice of the coefficients k_i is usually determined by the problem under consideration.

Consider the Lyapunov function as

$$V = \frac{1}{2g(\mathrm{x})}s^2 > 0 \tag{6}$$

If the designed control input u, such that x tracks x_r, according to the Lyapunov stability theory, makes $\dot{V}$ negative, then the trajectory of the system state would be driven and gets attracted to $s = 0$ and continues to slide till the origin is reached if $s\dot{s} < 0$.

Differentiation of V along the trajectories gives

$$\dot{V} = s\dot{s} = s\left(\sum_{i=1}^{n-1} k_i e_{i+1} + \hat{f}(\mathrm{x}) + \Delta\hat{f}(\mathrm{x}) + \eta(t) + \hat{g}(\mathrm{x})u(t) - x_r^{(n)}\right) \tag{7}$$

Then the control input u is chosen as sum of the equivalent control, u_{eq} and switching control u_{sw} which is expressed as $u = u_{eq} + u_{sw}$,

$$u_{eq} = \frac{1}{\hat{g}(\mathrm{x})}\left(-\sum_{i=1}^{n-1} k_i\, e_{i+1} - \hat{f}(\mathrm{x}) - \Delta\hat{f}(\mathrm{x}) - \eta(t) + x_r^{(n)}\right) \tag{8}$$

In general the terms $\Delta\hat{f}(\mathrm{x})$ and $\eta(t)$ are unknown and the modified equivalent control input is

$$u_{eq} = \frac{1}{\hat{g}(\mathrm{x})}\left(-\sum_{i=1}^{n-1} k_i e_{i+1} - f(\mathrm{x}) + x_r^{(n)}\right) \tag{9}$$

The switched control term is

$$u_{sw} = -\frac{k_s}{\hat{g}(\mathrm{x})}\mathrm{sgn}(s) \tag{10}$$

where

$$\mathrm{sgn}(s) = \begin{cases} \dfrac{|s|}{s} \text{ or } \dfrac{s}{|s|}; & s \neq 0 \\ 0; & s = 0 \end{cases} \tag{11}$$

and implies that $\underset{t\to\infty}{Lt}\ s = 0$ and hence $\underset{t\to\infty}{Lt}\ \mathrm{e} = 0$.

The control input (8) with (9) and (10) guarantees the convergence of state trajectory to the sliding function $s = 0$ from any initial state.

3.2. **Fuzzy sliding mode control.** The target of the FSMC is to fulfill the objective of SMC, i.e., to design a control input so that the condition on the sliding mode is satisfied. A fuzzy sliding surface replaces the switching term u_{sw} given in (10) by a fuzzy inference system as shown in Figure 4.

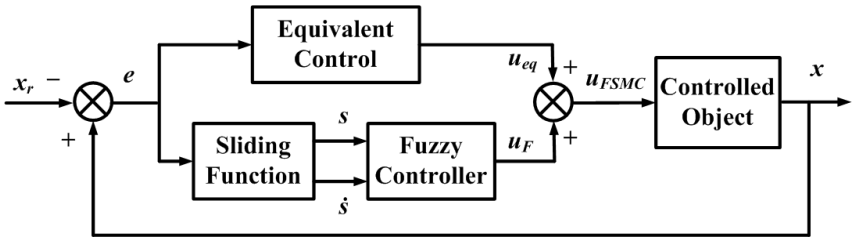

FIGURE 4. Block diagram of the FSMC

The two input variables to the fuzzy controller are the sliding function s and its derivative $\dot{s}$ and output is an equivalent control part.

In the control system, the final control u_{FSMC} becomes

$$u_{FSMC} = u_{eq} + u_F = u_{eq} + k_F u_{sw} \tag{12}$$

with fuzzy switching term

$$u_{sw} = -\frac{1}{g(\mathrm{x})} FC(s, \dot{s}) \mathrm{sgn}(s) \tag{13}$$

where k_F is the normalization factor and $FC(s, \dot{s})$ is the fuzzy decision function.

The fuzzy membership functions of inputs and the output $(s, \dot{s}, u_{sw})$ are shown in Figure 5, with five sets NS (negative small), ZE (zero), PS (positive small) with triangular shaped

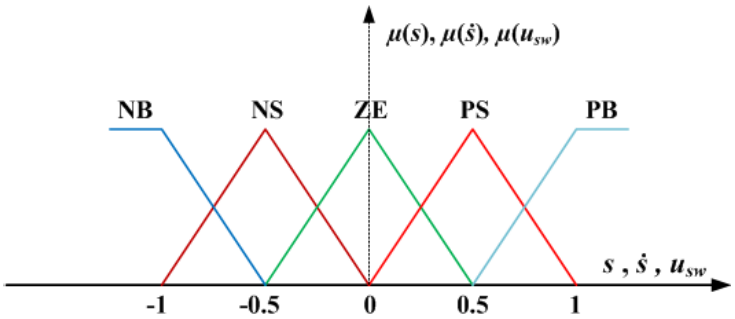

FIGURE 5. The fuzzy partitions of input and output variables

TABLE 1. Fuzzy decision rule matrix

u_{sw}		s				
		NB	NS	ZE	PS	PB
$\dot{s}$	NB	NB	NB	NB	NS	ZE
	NS	NB	NB	NS	ZE	PS
	ZE	NB	NS	ZE	PS	PB
	PS	NS	ZE	PS	PB	PB
	PB	ZE	PS	PB	PB	PB

functions and NB (negative big), PB (positive big) with S-shaped functions. The resulting 25 fuzzy decision rules are represented in Table 1. The outputs of FIS are defuzzified using centroid method to obtain the fuzzy control u_F.

3.3. **Radial force and torque control of BSRM.** The rotor radial force control in 2-DOF is achieved by generating force commands F_x^* and F_y^* as outputs of closed-loop FSMC controllers with displacement error as input. The displacement sensors located in four directions detect the rotor position and an encoder senses the rotor angular displacement. Using the generated force commands, two radial force poles one in each direction are selected for any rotor position and their currents are regulated by the asymmetric converter using PWM pulses. The motor speed is regulated by controlling torque winding current using an FSMC controller, with speed error as input. The proposed FSMC control scheme is shown in Figure 6.

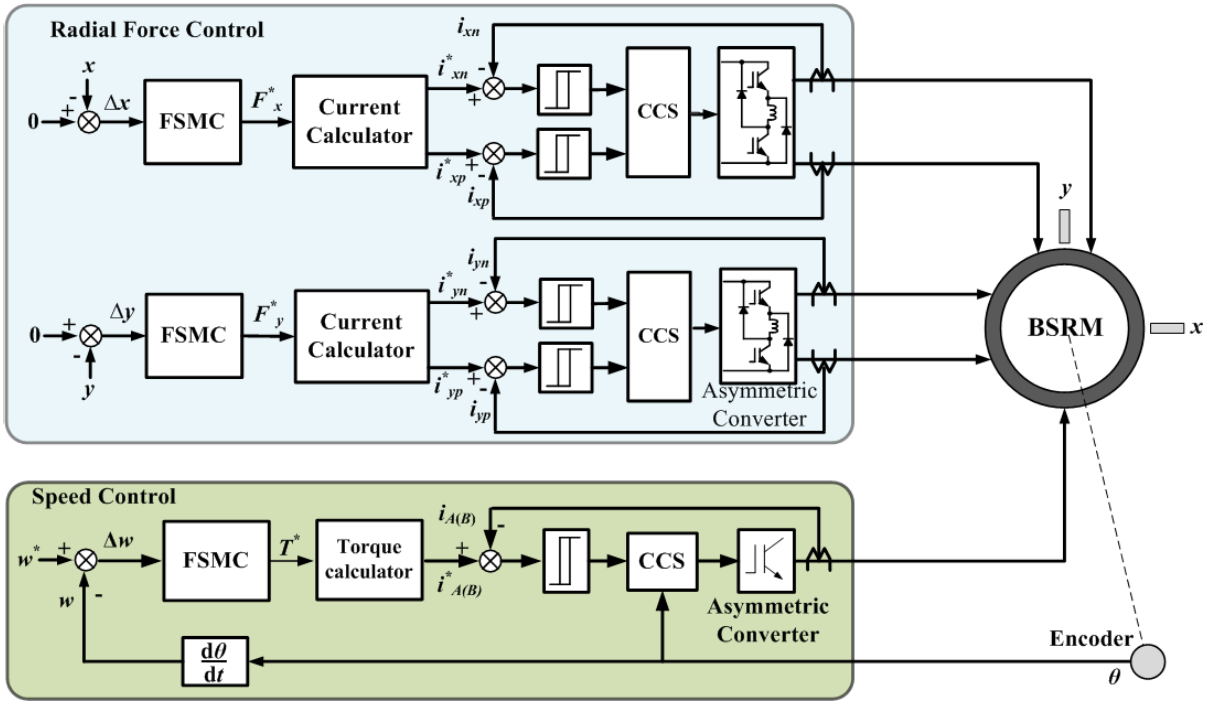

FIGURE 6. Block diagram of control scheme

4. **Experimental Results.** To validate the robustness of fuzzy sliding mode control, experiments have been performed on prototype hybrid pole type BSRM and the experimental test setup is shown in Figure 7. The FSMC and conventional SMC strategies are implemented with TMS320F2812 digital signal processor (DSP) which is compatible with Matlab/Simulink and includes 4 dual PWM channels, 4 ADCs, and a speed-encoder input. The encoder generates 2000 pulses per revolution with a supply voltage of 5V.

The appropriate sliding factors and fuzzy parameters of FSMC using the trial-and-error process are $k_1 = 1.5$, $k_s = 0.5$ and $k_F = 0.20$.

The experimental results of rotor displacements in both directions (x and y), and corresponding radial force currents during the startup process of the rotor levitation from the rest are shown in Figure 8. Since the rotor is initially resting at 80 μm in the $-x$ direction and 90 μm in the $+y$ directions, to levitate it, the winding currents i_{xp} and i_{yn} of radial force poles P_{xp} and P_{yn} are to be controlled according to the switching state rules.

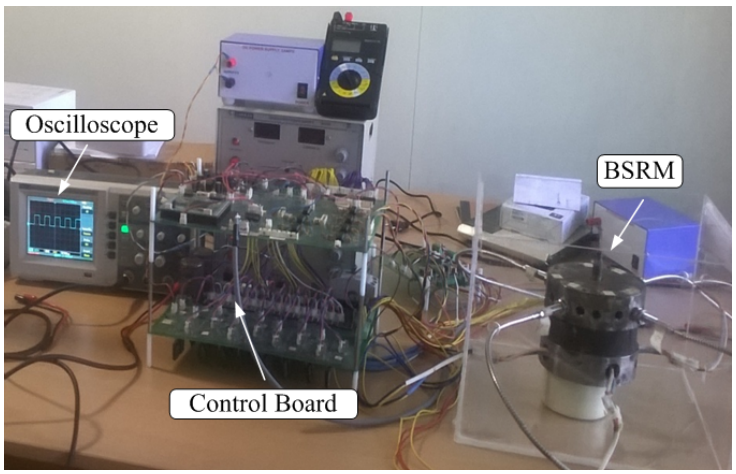

FIGURE 7. Experimental setup

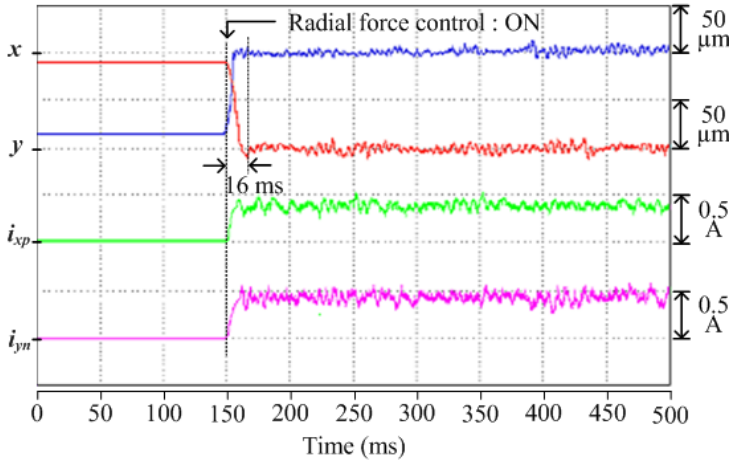

(a)

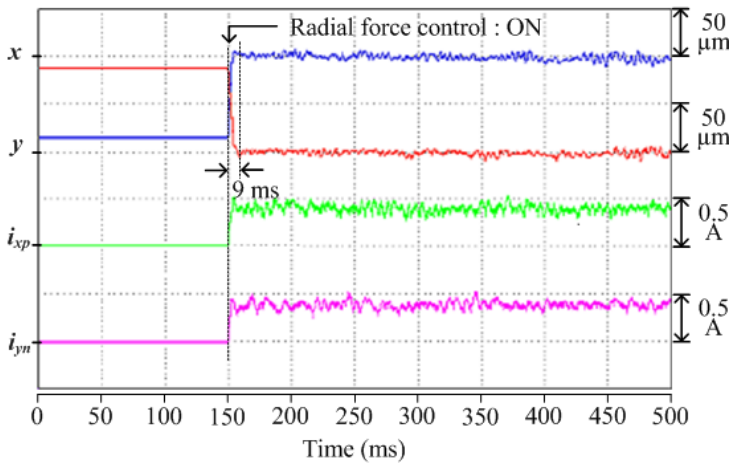

(b)

FIGURE 8. Displacements and radial force winding currents during rotor levitation from stand still condition (a) with conventional SMC and (b) with the proposed fuzzy SMC

From Figures 8(a) and 8(b), it can be inferred that when the radial force control is on at 150 ms, the rotor levitates and stays stable at the centre of the stator in 9 ms with FSMC when compared to 16 ms of conventional SMC. Besides, FSMC smoothens the rotor vibrations. The radial force winding currents i_{xp} and i_{yn} are also shown. Since the torque control is not applied, the rotor speed and phase currents are zero.

Figure 9 shows the results of the rotor radial displacements and speed when accelerating from 0 rpm to 1000 rpm with torque control is on at 1.5 s. Comparing Figures 9(a) and 9(b), it can be observed that the superiority of FSMC's in reducing chattering in the steady levitation of rotor with less ripples over SMC. Though the the rise time of speed response with FSMC is the same as that of SMC, the speed response with SMC is not as smooth as with FSMC. The rotor eccentricity with FSMC is within the region of ± 9 μm, which is obviously superior to that of ± 14 μm with SMC at the speed of 1000 r/min.

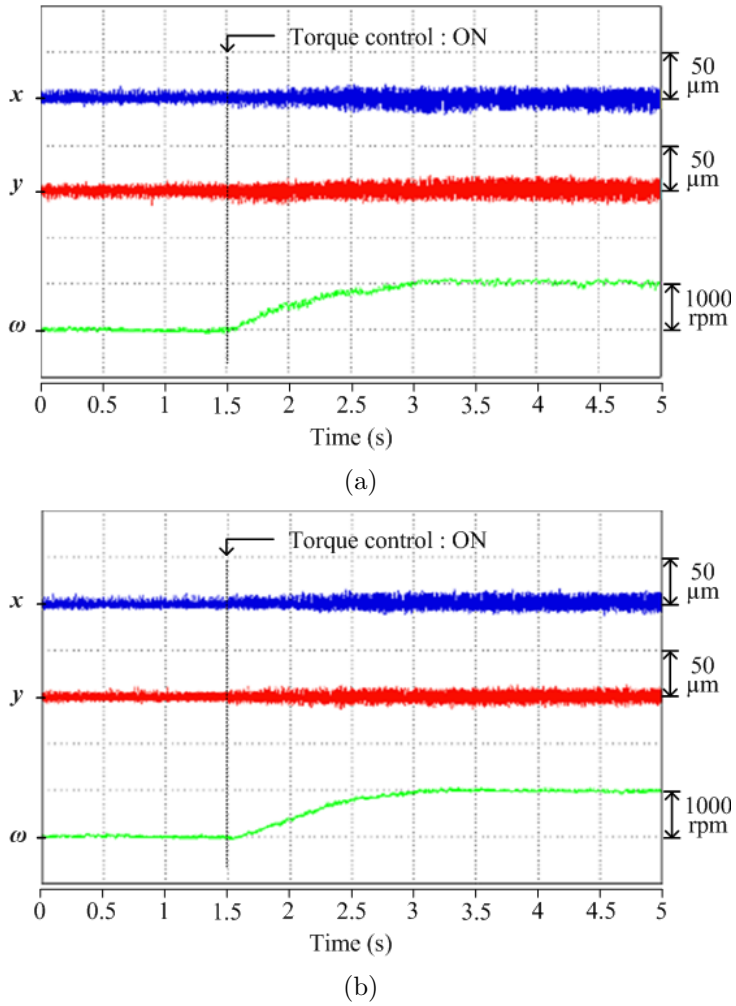

FIGURE 9. Rotor radial displacements and speed when accelerating from standstill (a) with conventional SMC and (b) with the proposed fuzzy SMC

Figure 10 shows the results of rotor vibration when an unknown impulse disturbance is applied at 150 ms. Figures 10(a) and 10(b) show the superiority of FSMC in suppressing rotor vibrations in x and y directions, and quick restoration to center position when compared to SMC. It can also be observed of no significant change in the rotor speed except at the moment of disturbance applied with FSMC.

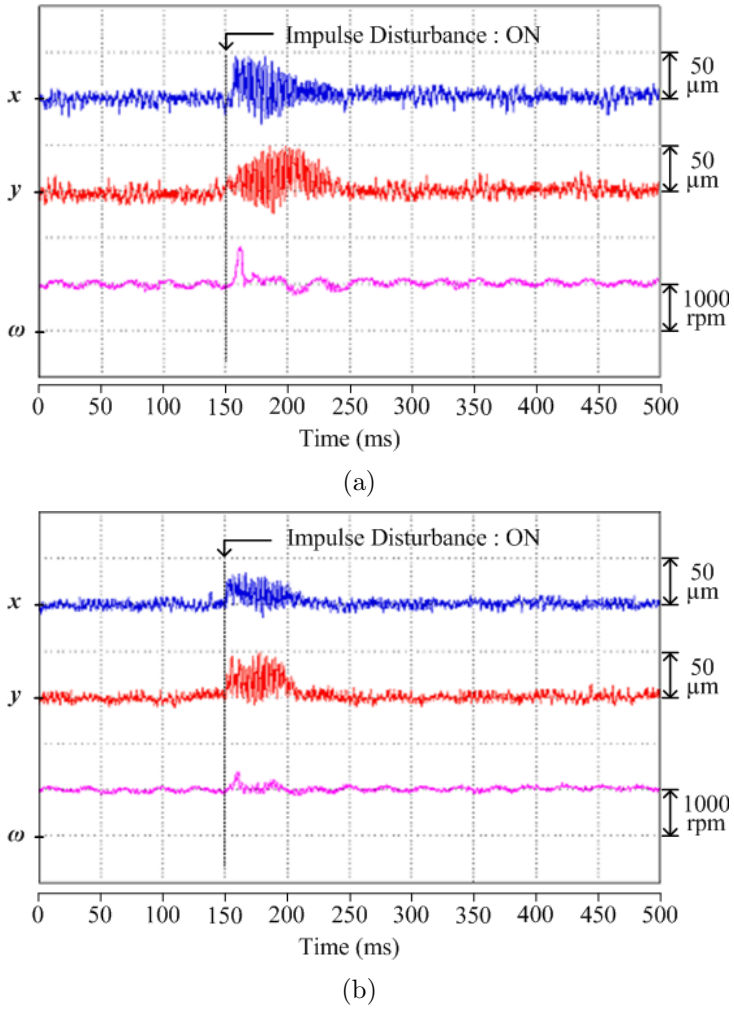

FIGURE 10. Rotor radial displacements and speed under impulse disturbance (a) with conventional SMC and (b) with the proposed fuzzy SMC

5. **Conclusions.** The BSRM is a multivariable and nonlinear system with unavoidable parameter variations and unmeasured disturbances. The important feature of hybrid pole type design is its inherent strong decoupling between the radial force and rotational force, which facilitates the independent control of rotor levitation and speed. This paper presents a control scheme combining the fuzzy logic with sliding mode control to control nonlinear vibrations caused by the nonlinearity of the radial force and eliminates chattering with enhanced performance. The experimental results demonstrate that unlike the conventional SMC, the rotor can be steadily levitated from standstill and accelerates to the desired speed with fewer vibrations with the FSMC.

REFERENCES

[1] R. Bosch, Development of a bearingless electric motor, *Proc. of ICEM*, Pisa, Italy, pp.373-375, 1988.
[2] J. Bichsel, The bearingless electrical machine, *Proc. of Int. Symp. Magn. Suspension Technol.*, Hampton, VA, USA, pp.561-573, 1991.
[3] K. Raggl, B. Warberger, T. Nussbaumer, S. Burger and J. W. Kolar, Robust angle-sensorless control of a PMSM bearingless pump, *IEEE Trans. Industrial Electronics*, vol.56, no.3, pp.2076-2085, 2009.
[4] M. Ooshima and C. Takeuchi, Magnetic suspension performance of a bearingless brushless DC motor for small liquid pumps, *IEEE Trans. Industry Applications*, vol.47, no.1, pp.72-78, 2011.

[5] T. Reichert, T. Nussbaumer and J. W. Kolar, Bearingless 300-W PMSM for bioreactor mixing, *IEEE Trans. Industrial Electronics*, vol.59, no.3, pp.1376-1388, 2012.
[6] B. Warberger, R. Kaelin, T. Nussbaumer and J. W. Kolar, 50-N.m/2500-W bearingless motor for high-purity pharmaceutical mixing, *IEEE Trans. Industrial Electronics*, vol.59, no.5, pp.2236-2247, 2012.
[7] X. Sun, L. Chen and Z. Yang, Overview of bearingless permanent magnet synchronous motors, *IEEE Trans. Industrial Electronics*, vol.60, no.12, pp.5528-5538, 2013.
[8] J. Asama, Y. Hamasaki, T. Oiwa and A. Chiba, Proposal and analysis of a novel single-drive bearingless motor, *IEEE Trans. Industrial Electronics*, vol.60, no.1, pp.129-138, 2013.
[9] S. Ayari, M. Besbes, M. Lecrivain and M. Gabsi, Effects of the airgap eccentricity on the SRM vibrations, *Proc. of Int. Conf. Elect. Mach. Drives*, pp.138-140, 1999.
[10] M. Takemoto, K. Shimada, A. Chiba and T. Fukao, A design and characteristics of switched reluctance type bearingless motors, *Proc. of the 4th Int. Symp. Magn. Suspension Technol.*, vol.NASA/CP-1998-207654, pp.49-63, 1998.
[11] M. Takemoto, A. Chiba, H. Suzuki et al., Radial force and torque of a bearingless switched reluctance motor operating in a region of magnetic saturation, *IEEE Trans. Industry Applications*, vol.40, no.1, pp.103-112, 2004.
[12] M. Takemoto, A. Chiba and T. Fukao, A new control method of bearingless switched reluctance motors using square-wave currents, *Proc. of the 2000 IEEE Power Engineering Society Winter Meeting*, Singapore, pp.375-380, 2000.
[13] L. Chen and W. Hofmann, Analytically computing winding currents to generate torque and levitation force of a new bearingless switched reluctance motor, *Proc. of the 12th EPE-PEMC*, pp.1058-1063, 2006.
[14] L. Chen and W. Hofmann, Performance characteristics of one novel switched reluctance bearingless motor drive, *Proc. of PCC*, Japan, pp.608-613, 2007.
[15] C. R. Morrison, M. W. Siebert and E. J. Ho, Electromagnetic forces in a hybrid magnetic-bearing switched-reluctance motor, *IEEE Trans. Magn.*, vol.44, no.12, pp.4626-4638, 2008.
[16] C. R. Morrison, Bearingless switched reluctance motor, *U.S. Patent 6 727 618*, 2004.
[17] H. Wang, Y. Wang, X. Liu and J. W. Ahn, Design of novel bearingless switched reluctance motor, *IET Elect. Power Appl.*, vol.6, no.2, pp.73-81, 2012.
[18] H. Wang, D.-H. Lee, T.-H. Park and J.-W. Ahn, Hybrid stator pole switched reluctance motor to improve radial force for bearingless application, *Energy Convers. Manag.*, vol.52, no.2, pp.1371-1376, 2011.
[19] J. Zhou, Z. Deng, X. Cao, C. Liu and C. Liu, Decoupling mechanism of torque and levitation-force control for 12/4 dual-winding bearingless switched reluctance motor, *International Conference on Electrical Machines and Systems (ICEMS)*, Chiba, Japan, pp.1-6, 2016.
[20] Z. Xu, D.-H. Lee and J.-W. Ahn, Comparative analysis of bearingless switched reluctance motors with decoupled suspending force control, *IEEE Trans. Industry Applications*, vol.51, no.1, pp.733-743, 2015.
[21] L. Chen and W. Hofman, Speed regulation technique of one bearingless 8/6 switched reluctance motor with simpler single winding structure, *IEEE Trans. Industrial Electronics*, vol.59, no.6, pp.2592-2600, 2012.
[22] X. Cao, Z. Deng and G. Yang, Independent control of average torque and radial force in bearingless switched-reluctance motors with hybrid excitations, *IEEE Trans. Power Electronics*, vol.24, no.5, pp.1376-1385, 2009.
[23] X. Cao, J. Zhou, C. Liu and Z. Deng, Advanced control method for single-winding bearingless switched reluctance motor to reduce torque ripple and radial displacement, *IEEE Trans. Energy Conversion*, 2017.